2016
International Symposium on Power Electronics,
Electrical Drives, Automation and Motion

Cooperative Control of Multi-Functional Inverters for Renewable Energy Integration and Power Quality Compensation in Micro-Grids

O. Deblecker, C. Stevanoni, F. Vallée
Electrical Engineering Division, Faculté Polytechnique, UMONS
Bd Dolez, 31, 7000 Mons
olivier.deblecker@umons.ac.be

***Abstract*—This paper deals with a methodology to cooperatively handle the power quality issues in a multiple-inverter-based micro-grid with communication. The micro-grid operates in the grid-connected mode, being partially supplied from the main network. The conservative power theory decomposition is used to deal with both the power enhancement and renewable power integration functions. A central controller manages the micro-grid operation by providing set-points to the local controllers of the inverters used to interface the renewable energy sources. Each set-point consist of two parts: one is used to compensate the power quality issues at the point of common coupling and the other corresponds to the active power/reactive energy references. Simulation results are shown considering, as an example, a three-phase three-wire micro-grid equipped with two inverters, together with unbalanced and nonlinear loads. Among the different analyzed situations, the possibility to supply reactive power at the point of common coupling is shown with a view to provide voltage support, which is an asset in the framework of smart distribution networks.**

Keywords—power quality; conservative power theory; cooperative control; multi-functional inverter

I. Introduction

Over the past several years, power distribution networks have been subject to important changes because of the proliferation of distributed energy resources [1]. Hence, this fact has been driving the integration of a large amount of information and communication technologies into these networks. Among the different aspects of this transition, micro-grid (portion of the distribution network) is regarded as a good choice to interface solar, wind and other renewable energy sources (RESs) into the network [2], [3]. However, due to the numerous converters and connected loads, the power quality issues, such as phase unbalance, reactive power and harmonic distortion, etc., have become the challenges which affect the stability and proper operation of the micro-grid. For improving the power quality of a micro-grid, some passive and active devices used in distribution networks were recommended [4], [5]. Yet, the inverters used to interface RESs into the network can be involved in the power quality enhancement function, aside to the renewable energy integration function (*i.e.* active power injection). Such kind of grid-tied inverter with ancillary service of power quality enhancement is usually referred to as multi-functional grid-tied inverter (MFGTI) (see, e.g., [6], [7], [8]). Hence, extra power quality conditioners may no longer be essential in a multiple-inverter-based micro-grid allowing for costs reduction.

The conservative power theory (CPT) offers a consistent framework to approach micro-grid characterization and guide the power quality service of the MFGTIs [9]. Indeed, this theory proposes an orthogonal decomposition of currents and powers in the stationary frame, according to terms which are directly related to specific physical phenomena. So, each disturbing cause (phase unbalance, waveform distortion, etc.) can be identified and eliminated independently from the others, allowing for selective power quality compensation as shown in [10], [11]. More recently, a single-phase inverter control strategy for distributed generation systems has been proposed based on the CPT [12]. This theory has also been used for active shunt compensation to provide reactive compensation and harmonic filtering in [13] and the coordinated operation in a multiple-inverter based micro-grid with CPT supervisory control has been investigated in [14].

The objective of the present paper is to propose a methodology to cooperatively handle the power quality issues in a three-phase three-wire micro-grid comprising multiple MFGTIs, with communication from a central controller. In this context, the CPT decomposition is used to deal with both the power quality enhancement and renewable energy integration functions, which is a novelty. For reasons of availability and operation stability, the micro-grid is operated in grid-connected mode, being partially supplied from the main network. The micro-grid central controller (MGCC) simultaneously exchanges active power/reactive power references with the MFGTIs to ensure the safe and economic operation of the micro-grid. The capacity of each MFGTI used for power quality enhancement is limited and related to its working condition.

The remainder of this paper is organized as follows. In Section II, the CPT is briefly reviewed. Then, in Section III, the cooperative control scheme based on the CPT decomposition is exposed, together with the model and local controller of the MFGTIs. Finally, simulation results are presented in Section IV in order to validate the implemented control scheme under different scenarios. Among the different analyzed situations, it will be shown that the proposed methodology allows for simple adjustment of the reactive power exchanged at the PCC, which is another originality of this work.

978-1-5090-2067-6/16/$31.00 ©2016 IEEE

II. Brief Review of the Conservative Power Theory

The CPT is defined in the time domain, for general operating conditions, and can be applied to single- and polyphase systems, with or without neutral wire. The theory proposes an orthogonal decomposition of currents and powers in the stationary frame, according to terms which are directly related to specific physical phenomena such as average power transfer, reactive energy, phase unbalance and distortion.

Consider a M-phase network under periodic operation (period T), where $\underline{u}$, $\underline{i}$ and $\underline{\hat{u}}$ are, respectively, the M-dimensional vectors of phase voltages, currents and unbiased voltage time integrals (*i.e.* AC components of the phase voltage integrals) measured at a generic network node. According to the CPT, the instantaneous power (p) and the instantaneous reactive energy (w) are conservative quantities, independently of the voltage and current waveforms. With '∘' denoting the dot product of vectors, these are expressed as

$$p = \underline{u} \circ \underline{i} \quad , \qquad w = \underline{\hat{u}} \circ \underline{i} \tag{1}$$

The corresponding average active power (P_μ) and average reactive energy (W_μ) in each phase μ are defined as follows:

$$P_\mu = \langle u_\mu, i_\mu \rangle = \frac{1}{T}\int_0^T u_\mu i_\mu dt \quad \Rightarrow \quad P = \sum_{\mu=1}^{M} P_\mu \tag{2}$$

$$W_\mu = \langle \hat{u}_\mu, i_\mu \rangle = \frac{1}{T}\int_0^T \hat{u}_\mu i_\mu dt \quad \Rightarrow \quad W = \sum_{\mu=1}^{M} W_\mu \tag{3}$$

Then, using the CPT, the current i_μ in each phase can be decomposed according to its active and reactive components.

The *active current* $i_{a\mu}$ is the minimum phase current needed to convey the active power P_μ. It can be shown that such current has no impact on the reactive energy. It is expressed by

$$\begin{aligned} i_{a\mu} &= \frac{\langle u_\mu, i_\mu \rangle}{\|u_\mu\|^2} u_\mu = \frac{P_\mu}{U_\mu^2} u_\mu = G_\mu u_\mu \\ \Rightarrow \quad \mathbf{I}_a &= \sqrt{\sum_{\mu=1}^{M} I_{a\mu}^2} = \sqrt{\sum_{\mu=1}^{M} \left(\frac{P_\mu}{U_\mu}\right)^2} \end{aligned} \tag{4}$$

where G_μ represents the equivalent conductance of phase μ and $\|u_\mu\|$ (= U_μ) is the norm (rms value) of the phase voltage. Note that bold notation (here, *e.g.*, $\mathbf{I}_a$) refers to the collective rms value.

On the other hand, the *reactive current* $i_{r\mu}$ is the minimum phase current needed to convey the reactive energy W_μ. It is expressed by

$$\begin{aligned} i_{r\mu} &= \frac{\langle \hat{u}_\mu, i_\mu \rangle}{\|\hat{u}_\mu\|^2} \hat{u}_\mu = \frac{W_\mu}{\hat{U}_\mu^2} \hat{u}_\mu = B_\mu \hat{u}_\mu \\ \Rightarrow \quad \mathbf{I}_r &= \sqrt{\sum_{\mu=1}^{M} I_{r\mu}^2} = \sqrt{\sum_{\mu=1}^{M} \left(\frac{W_\mu}{\hat{U}_\mu}\right)^2} \end{aligned} \tag{5}$$

where B_μ is the equivalent reactivity of phase μ. The reactive current has no influence on the active power.

Hence, it remains a residual term, called *void current* $i_{v\mu}$, neither linked to P_μ nor to W_μ, defined by

$$i_{v\mu} = i_\mu - i_{a\mu} - i_{r\mu} \tag{6}$$

All the aforementioned current terms are orthogonal (decoupled) to each other. So, we have for the rms values

$$\begin{aligned} I_\mu &= \|i_\mu\| = \sqrt{I_{a\mu}^2 + I_{r\mu}^2 + I_{v\mu}^2} \\ \Rightarrow \quad \mathbf{I} &= \sqrt{\mathbf{I}_a^2 + \mathbf{I}_r^2 + \mathbf{I}_v^2} \end{aligned} \tag{7}$$

To identify the effects of load unbalance and supply voltage asymmetry, the current terms can also be decomposed into balanced and unbalanced components. For instance, the M-dimensional vectors of *balanced* active and reactive currents, denoted $\underline{i}_a^b$ and $\underline{i}_r^b$ respectively, are defined as the minimum currents needed to convey the total active power P and total reactive energy W at the given node

$$\underline{i}_a^b = \frac{P}{\sum_{\mu=1}^{M} U_\mu^2} = \frac{P}{\mathbf{U}^2}\underline{u} = G^b \underline{u} \quad \Rightarrow \quad \mathbf{I}_a^b = \frac{P}{\mathbf{U}} \tag{8}$$

$$\underline{i}_r^b = \frac{W}{\sum_{\mu=1}^{M} \hat{U}_\mu^2} = \frac{W}{\hat{\mathbf{U}}^2}\underline{\hat{u}} = B^b \underline{\hat{u}} \quad \Rightarrow \quad \mathbf{I}_r^b = \frac{W}{\hat{\mathbf{U}}} \tag{9}$$

where G^b and B^b are, respectively, the equivalent *balanced* conductance and the equivalent *balanced* reactivity.

The *unbalanced* active and *reactive* currents in each phase μ at the given node are defined by difference as follows:

$$i_{a\mu}^u = \left(G_\mu - G^b\right) u_\mu \ , \quad i_{r\mu}^u = \left(B_\mu - B^b\right) \hat{u}_\mu \tag{10}$$

The balanced and unbalanced current terms are orthogonal to each other. Thus:

$$\sum_{\mu=1}^{M} \left\langle i_{a\mu}^u, i_{a\mu}^b \right\rangle = 0 \quad \Rightarrow \quad \mathbf{I}_a^u = \sqrt{\mathbf{I}_a^2 - \mathbf{I}_a^{b\,2}} \tag{11}$$

$$\sum_{\mu=1}^{M} \left\langle i_{r\mu}^u, i_{r\mu}^b \right\rangle = 0 \quad \Rightarrow \quad \mathbf{I}_r^u = \sqrt{\mathbf{I}_r^2 - \mathbf{I}_r^{b\,2}} \tag{12}$$

and the global unbalanced phase currents are obtained by the sum of the unbalanced active and reactive components (which are orthogonal to each other as well) as

$$\underline{i}^u = \underline{i}_a^u + \underline{i}_r^u \quad \Rightarrow \quad \mathbf{I}^u = \sqrt{\mathbf{I}_a^{u\,2} + \mathbf{I}_r^{u\,2}} \tag{13}$$

The last step is to decompose the apparent power S in introducing different power terms linked to the above-defined current components. This gives

$$\begin{aligned} S^2 &= P^2 + Q^2 + N^2 + V^2 \\ &= \mathbf{U}^2\mathbf{I}_a^{b\,2} + \mathbf{U}^2\mathbf{I}_r^{b\,2} + \mathbf{U}^2\mathbf{I}^{u\,2} + \mathbf{U}^2\mathbf{I}_v^2 \end{aligned} \tag{14}$$

where P is the active power, Q the reactive power, N the unbalance power and V the void power.

Note that, from (9) and the definition of $\underline{Q}$ in (14), the reactive power can be expressed in terms of the reactive energy as follows:

$$Q = \frac{\mathbf{U}}{\hat{\mathbf{U}}} W \tag{15}$$

In (15), the reactive power Q is not conservative (unlike the reactive energy). In fact, as proved in [9], it depends on the local voltage distortion.

Finally, the power factor PF is defined as follows:

$$\mathrm{PF} = \frac{|P|}{S} \tag{16}$$

III. Cooperative Control Scheme

Now, the cooperative control scheme proposed for MFGTIs application in a three-phase micro-grid and based on the CPT decomposition is presented.

The principle diagram of a multiple-inverter-based micro-grid connected to a MV/LV substation is depicted in Fig. 1. The micro-grid is centrally controlled by a MGCC installed at the PCC. The MGCC manages the micro-grid operation by providing set-points to the MFGTIs local controllers. Each set-point consists of two parts. One part is used to compensate the power quality issues at the PCC and takes the form of a (instantaneous) complex power reference. The other part is utilized to ensure the safe and economic operation of the micro-grid (as suggested *e.g.* in [15]). It corresponds to the desired active power and reactive energy flows at the point of connection (POC) of each MFGTI.

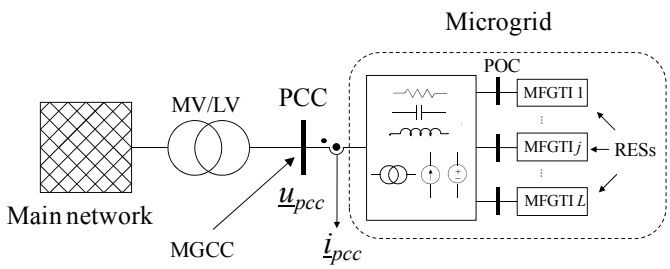

Fig. 1. Multiple-inverter-based micro-grid connected to the main network.

A. Complex Power Reference Calculation and Partitioning

To enhance the power quality at the PCC, the proposed methodology makes use of instantaneous complex power references calculated by the MGCC according to the block diagram shown in Fig. 2. Note that hereafter the superscript "p" will refer to the fundamental positive-sequence.

First, let us denote by $\underline{i}^*_{pcc}$, the vector of the three-phase currents taken as reference at the PCC. Comparing with the vector of the measured currents $\underline{i}_{pcc}$ absorbed at that node, the error signals vector $\underline{\varepsilon}$ (*i.e.* the vector of the currents to be compensated) is formed and amplified by a gain A_i in order to generate an internal reference.

Using the power theory reviewed above, the vector of the three-phase currents at the PCC can be decomposed into several terms as follows:

$$\underline{i}_{pcc} = \underline{i}_a^b + \underline{i}_r^b + \underline{i}^u + \underline{i}_v \tag{17}$$

where all the terms are orthogonal to each other.

Thus, for example, if the phase unbalance and harmonic distortion at the PCC have to be compensated (in this case, the switch K is on in Fig. 2), the reference vector $\underline{i}^*_{pcc}$ is put equal to the balanced active current and balanced reactive current terms as follows:

$$\underline{i}^*_{pcc} = \underline{i}^{b*}_{a,pcc} + \underline{i}^{b*}_{r,pcc} \tag{18}$$

Using (8) and (9), these terms can easily be calculated from the measured phase voltages (vector $\underline{u}_{pcc}$) and their unbiased voltage time integrals (vector $\underline{\hat{u}}_{pcc}$), provided that the total active power P_{pcc} and the total reactive energy W_{pcc} at the PCC are known (such quantities can be measured by simple instrumentation). Hence, the error signals vector $\underline{\varepsilon}$ is expressed as $-(\underline{i}^u+\underline{i}_v)$. It is worth noting that if the reactive energy must be compensated as well (switch K is off in Fig. 2), then the balanced reactive current term vanishes from (18) and the error signals vector becomes $-(\underline{i}_r^b+\underline{i}^u+\underline{i}_v)$.

Second, consider the complex power defined from the instantaneous power and reactive energy (*i.e.* the conservative quantities in the CPT). With j the imaginary number and $\omega(=2\pi/T)$ the fundamental angular frequency, the complex power reference at the PCC is written as

$$\bar{s}^* = p^* + j\omega w^* \tag{19}$$

where

$$p^* = \underline{u}^p_{pcc} \circ A_i \underline{\varepsilon}\ , \quad w^* = \underline{\hat{u}}^p_{pcc} \circ A_i \underline{\varepsilon} \tag{20}$$

As it can be noticed, it is the fundamental positive-sequence of the three-phase voltages and that of their unbiased time integrals which are used to evaluate the complex power in terms of the reference quantities p^* and w^*. This is justified by the fact that the MFGTIs cannot compensate for the voltage asymmetry and/or distortion caused by the main network.

Finally, the complex power reference based on conservative quantities must be partitioned among the MFGTIs, each being assigned a weighting coefficient α_j

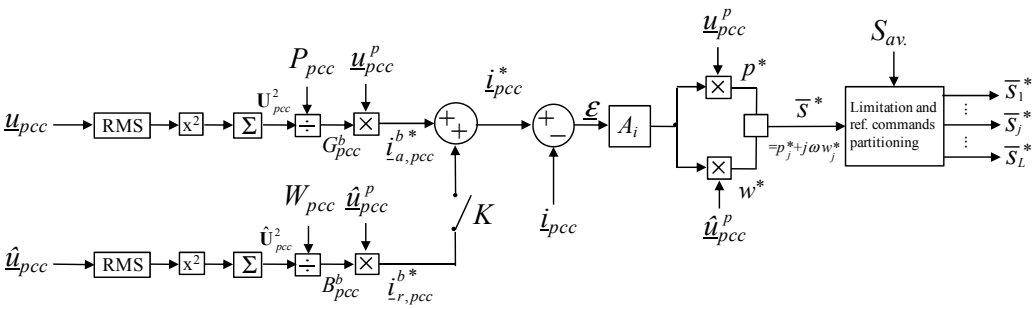

Fig. 2. Block diagram of the MGCC operation (instantaneous complex power commands calculation).

(defined, *e.g.*, as the ratio of its rated power to the total power capability)

$$\bar{s}^* = \sum_{j=1}^{L} \bar{s}_j^* = \sum_{j=1}^{L} \alpha_j \bar{s}^*, \text{ with } \sum_{j=1}^{L} \alpha_j = 1 \qquad (21)$$

Then, the MGCC downloads the individual complex power references to the MFGTIs local controllers. Of course, prior to that, it is important to verify that the norm of the complex power reference calculated by (19) does not exceed the total available compensation capability $S_{av.}$.

B. Inverter Control and Reference Currents Generation

The RESs are connected to the micro-grid by means of MFGTIs. Each MFGTI includes a typical two-level pulse width-modulation (PWM) converter with an output LCL filter, as shown in Fig. 3. The dc-link of the MFGTI is assumed as a dc voltage source V_d.

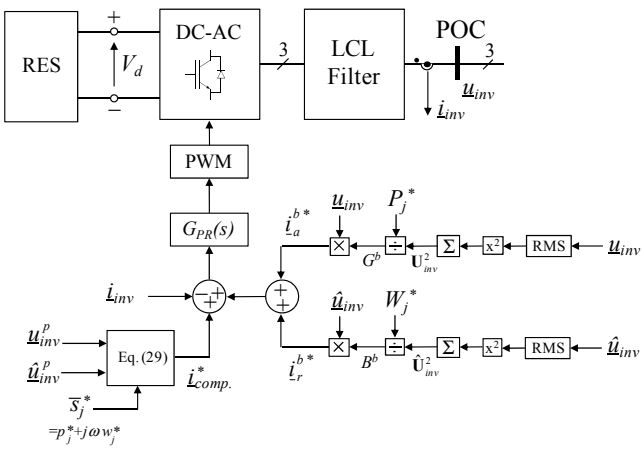

Fig. 3. Inverter-interfaced RES and block diagram of the local controller operation.

The inverter primary local controller is responsible for tracking the desired currents (vector $\underline{i}^*_{inv}$) at the POC, which consist of three parts as follows:

$$\underline{i}^*_{inv} = \underline{i}^{b*}_a + \underline{i}^{b*}_r + \underline{i}^*_{comp.} \qquad (22)$$

The first part is used to track the reference active power P_j^* sent by the MGCC to the local controller (say here that of the j-th inverter). Thus, the balanced active current term is written as

$$\underline{i}^{b*}_a = G^b \underline{u}_{inv} \qquad (23)$$

where $\underline{u}_{inv}$ is the measured instantaneous voltages at the POC of the MFGTI and G^b is the equivalent balanced conductance which, according to the CPT (see (8)), can be expressed as

$$G^b = \frac{P_j^*}{\mathbf{U}_{inv}^2} \qquad (24)$$

Similarly, the second part is used to track the reference reactive energy W_j^*. The corresponding balanced reactive current term is then written as

$$\underline{i}^{b*}_r = B^b \hat{\underline{u}}_{inv} \qquad (25)$$

where, from (9), the equivalent balanced reactivity can be calculated by

$$B^b = \frac{W_j^*}{\hat{\mathbf{U}}_{inv}^2} \qquad (26)$$

The third part is utilized to compensate the power quality issues at the PCC. For this purpose, the complex power reference sent to the MFGTI local controller must be transformed into reference three-phase currents (that is, the vector $\underline{i}^*_{comp.}$), which can be done as follows.

For the j-th inverter, the following reference quantities can be defined

$$p_j^* = \underline{u}^p_{inv} \circ \underline{i}^*_{comp.}, \quad w_j^* = \hat{\underline{u}}^p_{inv} \circ \underline{i}^*_{comp.} \qquad (27)$$

where $\underline{u}^p_{inv}$ is the vector of the positive-sequence phase voltages measured at the POC.

If it is assumed that the system is three-phase, three-wire (no zero sequence current terms), we have:

$$\sum_{\mu=1}^{3} i^*_{comp.,\mu} = 0 \qquad (28)$$

and thence the sought reference vector can be obtained by matrix inversion, simply as

$$\underline{i}^{*}_{comp.} = \begin{pmatrix} u_1 & u_2 & u_3 \\ \hat{u}_1 & \hat{u}_2 & \hat{u}_3 \\ 1 & 1 & 1 \end{pmatrix}^{-1} \begin{pmatrix} p^{*}_{j} \\ w^{*}_{j} \\ 0 \end{pmatrix} \tag{29}$$

where, to lighten the notation

$$(u_1, u_2, u_3) \equiv \underline{u}^{p}_{inv}\,, \quad (\hat{u}_1, \hat{u}_2, \hat{u}_3) \equiv \underline{\hat{u}}^{p}_{inv}$$

In order to track the reference current $\underline{i}^{*}_{inv}$, several control techniques are available in the literature (see, *e.g.*, [16] for a review). In this contribution, a multiple proportional-resonant (PR) regulator is implemented in the stationary frame, along with a modulator to create the duty cycles for the PWM pattern [17].

As an example, the schematic of the current-tracking control structure for phase 1 is shown in Fig. 4 where K_{PWM} ($= V_d/2$) is the equivalent gain of the MFGTI. These are supplied by a 750 V dc input voltage. For simplicity, the output LCL filter normally used to mitigate the harmonics generated by the inverter is replaced by a three-phase filter inductor (inductance per phase $L = 7.7$ mH). Hence, the transfer function G(s) deduced from the dynamic characteristic of the current $i_{inv,1}$ across the filter inductor is expressed as

$$G(s) = \frac{1}{r_d + Ls} \tag{30}$$

where s the Laplace variable and r_d represents the equivalent parasitic resistor.

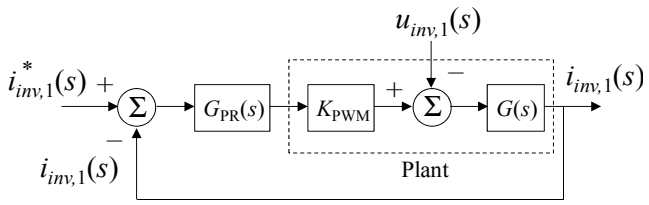

Fig. 4. Structure of the current-tracking control loop with multiple PR regulator (in phase 1).

The design of the controller can be conducted as follows. The transfer function of a multiple PR regulator is given by

$$G_{PR}(s) = K_p + \sum_{h=1,3,5,\ldots} \frac{K_{i,h}\, s}{s^2 + 2\zeta\omega_h s + \omega_h^2} \tag{31}$$

where ω_h is the angular frequency of the h-th harmonic component; K_p and $K_{i,h}$ ($h = 1, 3, 5, 7, 9, 11$) are the proportional gain and integral gains of the PR regulator, respectively.

The relationship between the inputs and output of the current-tracking loop shown in Fig. 4 can be derived as

$$i_{inv,1}(s) = H_i(s)\, i^{*}_{inv,1}(s) + H_u(s)\, u_{inv,1}(s) \tag{32}$$

where

$$H_i(s) = \frac{G_{\mathrm{PR}}(s) K_{\mathrm{PWM}} G(s)}{G_{\mathrm{PR}}(s) K_{\mathrm{PWM}} G(s) - 1}$$
$$H_u(s) = \frac{-G(s)}{1 + G_{\mathrm{PR}}(s) K_{\mathrm{PWM}} G(s)} \tag{33}$$

Since $G_{\mathrm{PR}}(s)$ has a very large gain at each resonant angular frequency ω_h, the term $H_u(s)$ in (32) can be neglected. Therefore, in practice, it is not necessary to have the voltage feed-forward in the current control loop.

The open-loop and close-loop Bode diagrams of the MFGTI with a multiple PR controller are shown in Fig. 5a and 5b, where $\zeta\omega_h$ = 10 rad/s, $K_p = 2.5$ and $K_{i,h} = 400$ (for every harmonic order h). With these values, it can be seen that appropriate zero-error tracking performance can be achieved at the resonant angular frequencies, which is due to the high gain and zero phase-shift features of the multiple PR controller at such frequencies.

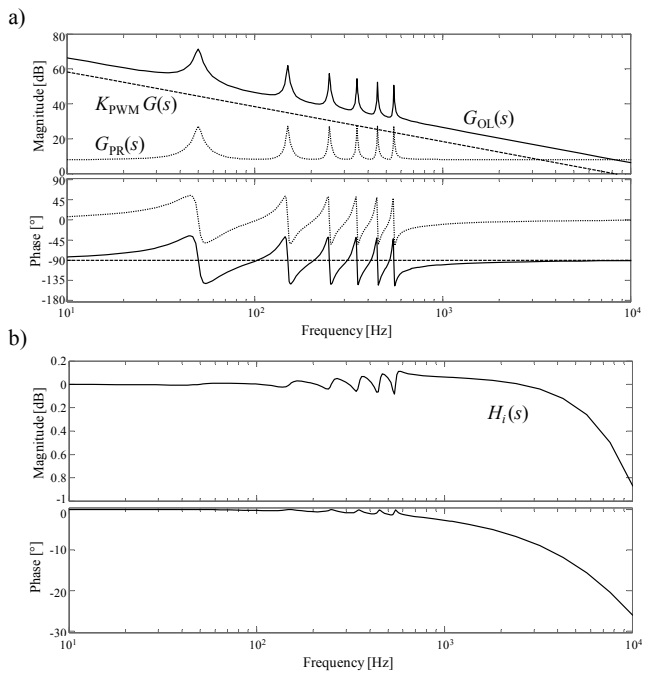

Fig. 5. Bode diagrams of the MFGTI. a) Open-loop transfer function: $G_{\mathrm{OL}}(s) = G_{\mathrm{PR}}(s) K_{\mathrm{PWM}} G(s)$ and b) close-loop transfer function $H_i(s)$.

IV. Application Example

A. Simulated Micro-Grid

The proposed methodology has been tested by simulation for the three-phase three-wire micro-grid shown in Fig. 6, including unbalanced and distorting loads, a transformer, transmission lines, and two MFGTIs rated 20 and 40 kVA respectively. This low-voltage network is inspired from reference [18]. The supply voltages fed at the PCC are 400 V rms, 50 Hz (line-to-line, positive-sequence components), affected by an asymmetry of 2 % (negative-sequence components). The proposed system was simulated by using a co-simulation with Simulink and PSIM softwares.

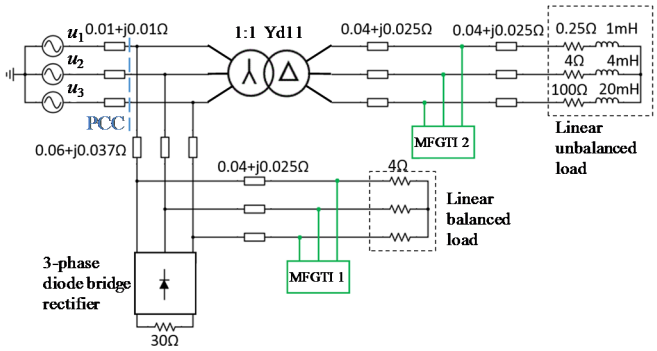

Fig. 6. Simulated micro-grid

B. *Simulation Results With Full Compensation*

First, the cooperative control scheme is applied to compensate for the load unbalance, reactive power and harmonic distortion at the PCC (full compensation). It is supposed that the power capability of each MFGTI is fully available for compensation (*i.e.*, for each, the reference active power and the reference reactive energy are set to zero). Moreover, in this work, the complex power reference is partitioned according to a criterion that accounts only for the power ratings of the MFGTIs (*i.e.* that, in (21), the weighting coefficients α_1 and α_2 are chosen equal to 1/3 and 2/3, respectively).

The micro-grid operation is first analyzed without any type of compensation. At $t = 0.7$ s, the cooperative control is activated with a unitary gain A_i. Then, at $t = 1.4$ s, the gain is increased to 15 so as to enhance the compensation effect. The simulation results are shown in Fig. 7 and 8.

As can be seen in Fig. 7, the unbalance (N), reactive (Q) and void (V) powers at the PCC are significantly reduced under the compensating action of the MFGTIs, provided that the gain is sufficient. The corresponding time behaviours of the power factor PF (given by (16)) and the unbalance factor UF (defined as the ratio between the negative- and positive-sequence components of the currents at the PCC) are represented in Fig. 8. The expected values (near to 1 and zero, respectively) are reached after $t = 1.4$ s, reflecting the power quality improvement. The total harmonic distortion (THD_i) of the three-phase currents at the PCC is reported in Table I at the different steps of the simulation. The time waveforms of these currents, without and with compensation (taking $A_i = 15$), are also shown in Fig. 9, allowing for a qualitative appreciation.

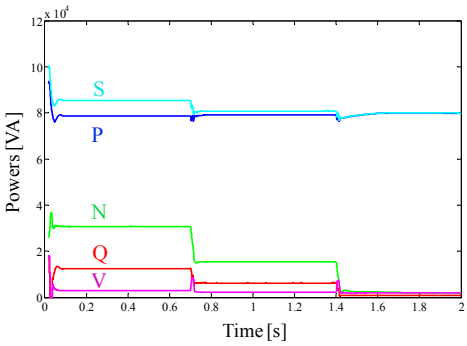

Fig. 7. Time behaviour of the power terms at the PCC.

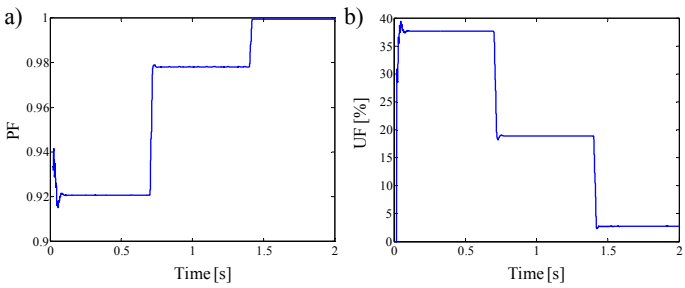

Fig. 8. Time behaviour of a) the power factor and b) the unbalance factor at the PCC.

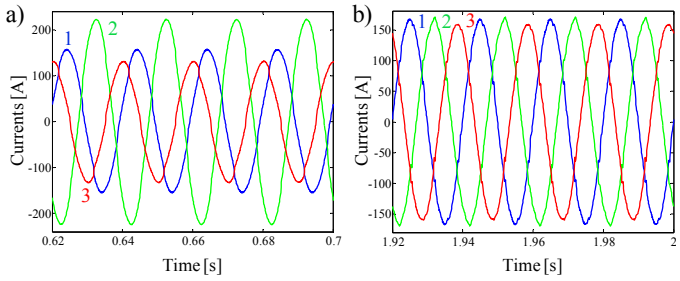

Fig. 9. Time waveforms of the currents at the PCC: a) without and b) with compensation.

TABLE I. TOTAL HARMONIC DISTORSION OF THE CURRENTS AT THE PCC

	Phase 1	Phase 2	Phase 3
Without compensation	3.49 %	2.47 %	4.69 %
With $A_i = 1$	1.89 %	1.56 %	2.12 %
With $A_i = 15$	1.43%	1.63 %	1.86 %

In order to assess the influence of the gain on the effectiveness of the compensation, the previous simulation has been repeated for different values of A_i. The results are reported in Table II. As it can be noticed, a gain of 15 yields a good trade-off between the reduction of the undesirable effects and the total occupied capacity $S_{comp.}$ for power quality compensation. Note also that the unbalance factor cannot be decreased to lower than approximately 2 %, which is a consequence of the asymmetry of the supply voltage itself at the PCC.

TABLE II. INFLUENCE OF THE GAIN A_I

Gain value	***Q*** **[VAR]**	***N*** **[VA]**	***V*** **[VA]**	**UF [%]**	**PF**	$S_{comp.}$ **[VA]**
0 (no comp.)	12434	30792	2852	37.7	0.920	0
1	6219	15423	2190	18.9	0.978	9815
2	4172	10292	2024	12.5	0.990	13158
5	2091	5152	1800	6.3	0.997	16667
10	1142	2808.7	1849	3.7	0.999	18759
15	**792**	**1950**	**1980**	**2.8**	**0.999**	**20253**
20	599	1514	2066	2.4	0.999	21675
30	403	1088	2202	2.2	0.999	25748

C. Simulation Results With Active Power Injection

In this scenario, we consider the injection of active power by the MFGTIs at $t = 0.5$ s. The cooperative control is simultaneously applied at $t = 1$ s to compensate for all the undesirable effects at the PCC (the gain A_i is successively equal to 1 and 15 as in the previous case). Fig. 10a shows the time behaviour of the different power terms. For each inverter, the corresponding local controller applies a step of active power reference P_j^* ($j = 1,2$) from zero to 10 kW and from zero to 20 kW, respectively.

After a transient of about two fundamental time periods, this yields a reduction of 30 kW (= 10+20 kW) at the PCC (see Fig. 10b for a zoom). The other power terms are not affected in steady state thanks to the decoupling inherent to the CPT decomposition. The power quality is clearly improved at the PCC, once the MFGTIs activate their compensation services.

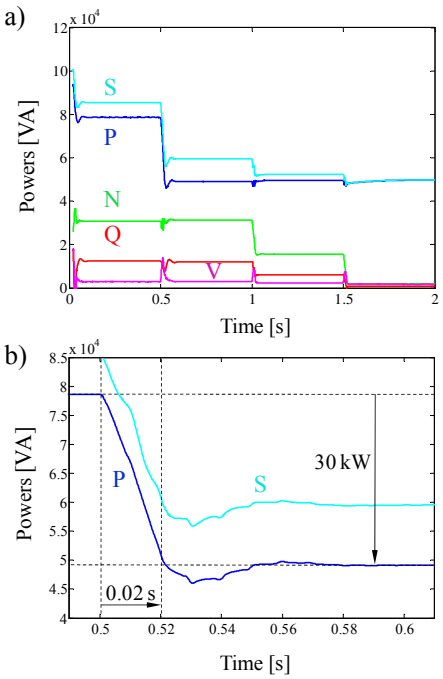

Fig. 10. a) Injection of 30 kW by the MFGTIs, plus full compensation; b) zoom on the response to the step of active power references at 0.5 s.

D. Supply/absorption of reactive power at the PCC

Finally, with a view to provide voltage support to the main distribution system, the possibility of using the cooperative control scheme to supply or absorb a given amount of reactive power (Q^*_{pcc}) at the PCC is shown. To that end, the reference vector $\underline{i}^*_{pcc}$ is put equal to the sum of the balanced active and reactive current terms as follows:

$$\underline{i}^*_{pcc} = \underline{i}^b_a + B^b_{pcc}\,\underline{\hat{u}}_{pcc} \tag{34}$$

where from (9) and (15), the balanced reactivity is written

$$B^b_{pcc} = \frac{W^*_{pcc}}{\hat{\mathbf{U}}^2_{pcc}} = \frac{Q^*_{pcc}}{\mathbf{U}_{pcc}\hat{\mathbf{U}}_{pcc}} \tag{35}$$

Hence, the MGCC sends the reactive energy references to the MFGTIs local controllers according to a given strategy, provided that

$$W^*_{pcc} = \sum_{j=1}^{L} W^*_j \tag{36}$$

Note that the sign of Q^*_{pcc} is positive or negative, according to the direction of the reactive power flow (absorption from or injection into the main network, respectively).

For the purpose of illustration, we consider the situation when the cooperative control is activated at $t = 0.5$ s with a gain $A_i = 15$ and $Q^*_{pcc} = 0$. The active power reference is equal to zero for each inverter during the entire simulation time interval. At $t = 1$ s, a (negative) step of reactive power reference Q^*_{pcc} is applied, from zero to –20 kVAR. In this example, it is assumed that the references of reactive energy are distributed equally among the two MFGTIs, *i.e.* $W^*_j = W^*_{pcc}/2$ for $j = 1,2$.

The time behaviour of the different power terms is represented in Fig. 11a. The reactive power at the PCC decreases from +12.4 kVAR initially to approximately –20 kVAR. A zoom is shown in Fig. 11b in order to visualize the transient (about one fundamental period). The unbalance and void powers are close to zero from the moment the MFGTIs activate their compensation services.

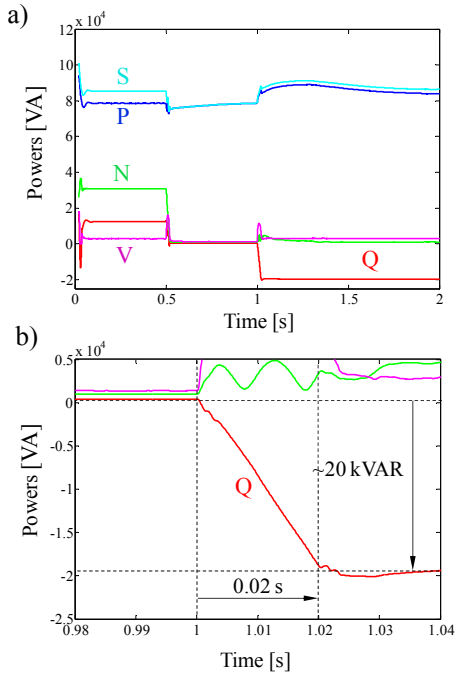

Fig. 11. a) Supply of 20 kVAR to the main network, compensation of the unbalance and void powers; b) zoom on the response to the step of reactive power reference at 1 s.

V. Conclusion

In this paper, a methodology has been proposed to cooperatively handle the power quality issues in a multiple-inverter-based micro-grid with communication. The micro-grid operates in the grid-connected mode, being partially

supplied from the main network. The CPT decomposition, defined for general operating conditions, has been advantageously used to deal with both the power quality enhancement and the renewable energy integration functions. This theory proposes an orthogonal decomposition of currents and powers in the stationary frame, according to terms which are directly related to specific physical phenomena (average power transfer, phase unbalance, etc.). Hence, each power term can be compensated independently from the others. As an application example, a three-phase micro-grid including unbalanced and nonlinear loads, together with two MFGTIs, has been simulated and the cooperative control scheme applied in different situations (full compensation, active power injection from the MFGTIs, etc.). It has been shown also that, defining adequately the balanced reactive current term at the PCC, the supply (or absorption) of reactive power to the main distribution network can be easily adjusted, which is an asset in the framework of smart distribution networks.

REFERENCES

[1] M. Liserre, T. Sauter, and J. Y. Hung, "Future energy systems," *IEEE Ind. Electron. Mag.*, pp. 18-37, Mar. 2010.

[2] P. C. Loh, et al., "Autonomous operation of distributed storages in microgrids," *IET Power Electron.*, vol. 7, n°1, pp. 23-30, Jan. 2014.

[3] I. U. Nutkani, P. C. Loh, F. Blaabjerg, "Cost-based droop scheme with lower generation costs for microgrids," *IET Power Electron.*, vol. 7, n°5, pp. 1171-1180, May 2014.

[4] M. Prodanovic, T. C. Green, "High-quality power generation through distributed control of a power park microgrid," *IEEE Trans. Ind. Electron.*, vol. 53, n°5, pp. 1471-1482, Oct. 2006

[5] B. Rahmani, M. T. Bina, "Reciprocal effects of the distorted wind turbine source and the shunt active power filter: full compensation of unbalance and harmonics under 'capacitive non-linear load' condition," *IET Power Electron.*, vol. 6, n°8, pp. 1668-1682, Sep. 2013.

[6] Z. Chen, F. Blaabjerg, J. K. Pedersen, "A multi-functional power electronic converter in distributed generation power systems," in *Proc. of the IEEE Annual Power Electron. Spec. Conf.*, Recife, Brazil; Jun. 2005.

[7] Z. Zeng, *et al.*, "Topologies and control strategies of multi-functional grid-connected inverters for power quality enhancement: a comprehensive review," Renew. Sustain. Energy Rev., vol. 24, pp. 223-270, Aug. 2013.

[8] Z. Zeng, *et al.*, "Objective-oriented power quality compensation of multi-functional grid-tied inverters and its application in micro-grids," *IEEE Trans. Power Electron.*, vol. 30, n°3, pp. 1255-1265, Mar. 2015.

[9] P. Tenti, H. K. Paredes, and P. Mattavelli, "Conservative power theory, a framework to approach control and accountability issues in smart microgrids," *IEEE Trans. on Power Electron.*, vol. 26, no. 3, Mar. 2011.

[10] P. Tenti, *et al.*, "Compensation of load unbalance, reactive power and harmonic distortion by cooperative operation of distributed compensators," in *Proc. 13th Eur. Conf. Power Electron. and Appl.*, Barcelona, Spain, Sep. 2009.

[11] H. Paredes, et al., "Harmonic, reactive and unbalance compensation by means of CPT framework," in Proc. Brazilian Power Electron. Conf., Bonio, Brazil, pp. 741-748, Sep. 2009.

[12] D. I. Brandão, *et al.*, "Inverter control strategy for DG systems bases on the conservative power theory," in *Proc. Energy Conversion Congress and Expo. (ECCE)*, Denver, USA, pp. 3283-3290, Sep. 2013.

[13] T. S. Haugan and E. Tedeschi, "Reactive and harmonic compensation using the conservative power theory," in *Proc. Tenth Intern. Conf. on Ecological Vehicles and Renewable Energies,* Nice, France, Oct. 2015.

[14] A. Mortizaei, *et al.*, "Coordinated operation in a multi-inverter based microgrid for both grid-connectd and islanded modes using conservative power theory," in *Proc. Energy Conversion Congress and Expo. (ECCE),* Montreal, Canada, pp. 4602-4609, Sep. 2015.

[15] J.M. Guerrero, et al., "Advanced control architectures for intelligent microgrids–Part I: Decentralized and hierarchical control," *IEEE Trans. Ind. Electron.*, vol. 60, n°4, pp. 1254-1262, Apr. 2013.

[16] M. Hojabri, *et al.*, "An overview on current control techniques for grid connected renewable energy systems," in *Proc. 2nd Int. Conf. Power and Energy Sys.*, pp. 119-126, 2012.

[17] M. Ebad and B.-M. Song, "Improved design and control of proportional resonant controller for three-phase voltage Source Inverter," in *Proc. Power Electron. and Machines in Wind Appl.* (PEMWA), Denver, USA, Jul. 2012.

[18] A. Costabeber, *et al.*, "Selective compensation of reactive, unbalance and distortion power in smart grids by synergistic control of distributed switching power interfaces", in *Proc. EPE'13 ECCE Europe*, Lille, France, Sep. 2013.